Biochemical Fixing and Activation Mechanisms of Amino Groups Deposited on the Surface and in the Depth of Polymeric Layers of the n[$SiO_{1.5}$-$(CH_2)_3NH_2$] Type Deposited on the Fe_3O_4 Nanoparticle Surface

PETRIŞOR ZAMORA IORDACHE[1]*, VASILE SOMOGHI[1], ION SAVU[1], NICOLETA PETREA[1], GEORGETA MITRU[1], RAZVAN PETRE[1], BOJIN DIONEZIE[2], VIOREL ORDEANU[3], ATENA HOTARANU[4], LUCIA MUTIHAC[4]

[1] Scientifical Research Center for NBC Defence and Ecology, 225 Olteniţei,041309, Bucharest,Romania

[2] Politehnica University of Bucharest – Biomaterials Research Center, 313, Spl. Independentei, 060042, Bucharest,Romania

[3] Medico-Military Scientifical Research Center, 37, C.A. Rosetti, 020012, Bucharest,Romania

[4] University of Bucharest, Department of Analytical Chemistry, 4-12, Regina Elisabeta Blvd., 030018, Bucharest,Romania

This paper presents the synthesis of complex nanostructures of the Fe_3O_4-n[$SiO_{1.5\gamma}$-$(CH_2)_3(NH_2)$]$(NH_2)_{n\delta}$-$(GL)_{n\varepsilon}$ type [Fe_3O_4 = magnetic core; n[$SiO_{1.5\gamma}$-$(CH_2)_3(NH_2)$] = coated layer; $(NH_2)_{n\delta}$-NH_2= surface and deep amino groups which play an important role in biochemical interfacing; $(GL)_{n\varepsilon}$ = exterior superficial glutaraldehyde layer]. These nanostructures have several interesting physical and chemical characteristics, such as: biochemical fixing without destructing the microorganisms on the Fe_3O_4-n[$SiO_{1.5\gamma}$-$(CH_2)_3(NH_2)$]$(NH_2)_{n\delta}$-$(GL)_{n\varepsilon}$ surface and the ability to differentiate the microorganisms in magnetic field, according to the mass and volume. In order to obtain superior biochemical fixing performances we have analysed and determined the chemical and physical distributional mechanisms of $(NH_2)_{n\delta}$ -NH_2 groups on the surface and in the depth of the above-mentioned nanostructure. For this purpose we have deduced the control equations according to the synthesis parameters, which triggers the growth of the silicone polymer layer and the distribution of the amino groups in its structure.

Keywords: Magnetite, coated nanoparticle, biochemical fixing, crosslinking molecules

The biochemical detection is a challenge from the point of view of the techniques and technologies involved in it. The classical specific biochemical tests (e.g., enzyme, metabolism, chromatography in thin layer, etc.) are the only ones which have a high degree of certainty of biostructural identification, but have the disadvantage of sequential and difficult determination. These tests will have positive results in hinting the biostructure type which is to be determined.

In the case of the analytical methods with high degree of sensitivity and prediction, of the GC, GC-MS, NMR type the analyses are carried out through degradations of molecular structures which constitute the determined structure. Moreover, this is equivalent with respect to the biochemical structural identity with the irreversibility of theoretical reconstruction of the real structure, therefore with the impossiblity of performing an identification.

Great attention has been paid nowadays to biochemical identification by means of nanostructures having physical and chemical properties inserted in a controlled manner and which can be monitored in the presence of external physical fields. The nanostructures with physical characterisics induced in a controlled manner in the chemical synthesis stage (e.g., magnetic moment, specific surface, specificity, strucure, etc.) have the advantage of the modelling of the component which is responsible for the biochemical fixing, keying and the subsequent control of the fixed biostructures, according to the proposed purpose (fig.1).

The present paper presents the controlled synthesis and biochemical activation of Fe_3O_4 [1] nanoparticles, their coating in polymeric layers of the n[$SiO_{1.5\gamma}$-$(CH_2)_3(NH_2)$]$(NH_2)_{n\delta}$ (**C1**) type and the determination of the physico-chemical control parametres of the obtained Fe_3O_4-n[$SiO_{1.5\gamma}$-$(CH_2)_3(NH_2)$]$(NH_2)_{n\delta}$-$(GL)_{n\varepsilon}$ (**C2**). The silicone polymer layer deposited and biochemically activated represents an acceptable option of organic and anorganic macrostructure retention, as pure magnetite has a low fixing chemical potential [2].

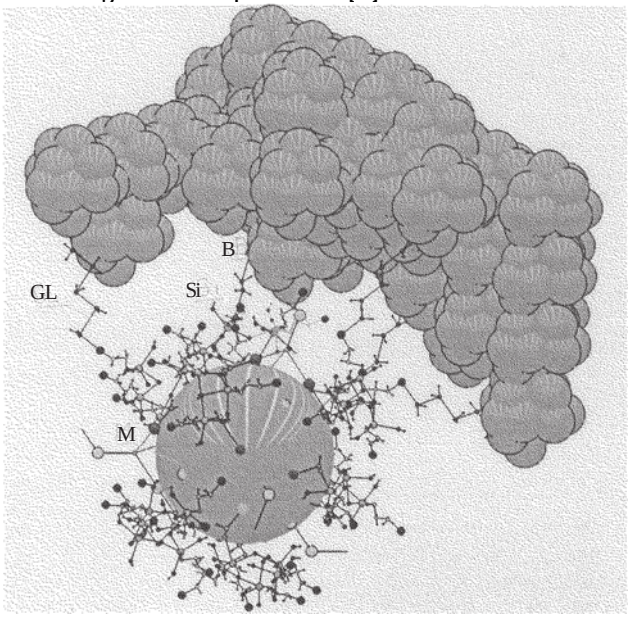

Fig.1. 3D model of crosslinking biostructure with molecular functional groups GL - glutaraldehyde, Si - n[$SiO_{1.5\gamma}$-$(CH_2)_3(NH_2)$] layer, B - glutaraldehyde crosslinked biostructure, M- Fe_3O_4 core

* *email: iordachezamora@yahoo.com; Tel.: 0726129158*

The availability of nanostructures which are efficient from the point of view of the fixing efficiency and of the specificity of the discrimination in external fields, which should have the physical and chemical characteristics previously mentioned, implies the detailed study of the rising mechanisms of the deposited polymeric layer, the disposal and the action of the groups responsible with biochemical fixing and the external control of nanoparticle parametres, essential for the proposed purpose.

Experimental part

The following reagents have been used for the Fe_3O_4 synthesis, stabilization and passivisation [3]: $FeCl_3$, $FeCl_2$ (Acros Organics); NH_3 (25%), HNO_3 (63%), (Reactivul Bucureşti); sodium citrate tribasic (Merck). The agitation was made with the LBS2-4.5L ultrasound bath (from FALC) with a maximum stirring rate of 55 KHz.

(3-aminopropyl)-triethoxysilane and absolute etilic alcohol have been used for the deposition of the C1 layer through self-condensation [4]. The biochemical activation has been carried out with glutaraldehyde (Merck).

The characterisitc X-ray spectra have been obtained by means of the ESEM Philips XL30 scanning electronic microscope which has the following working parametres: 25kV acceleration tension, 70 μA sample current , ESEM analysis mode, EDAX X radiation analyser.

The analysis of nanoparticle morphology and size has been carried out by means of the Philips S208 electronic microscope which has the following working parametres: 80 kV acceleration tension, 3 spot, 19 μA beam current and Olympus camera.

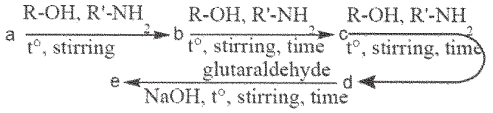

R-OH=Et-OH

R'-NH_2=(3-aminopropyl)-triethoxysilane

Scheme of the main stages of controlled chemical synthesis of Fe3O4 nanoparticles coated in polimer of the C1 type

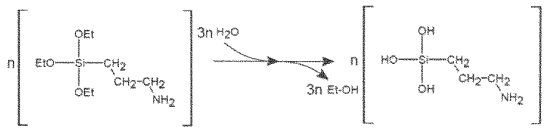

a. hydrolysis

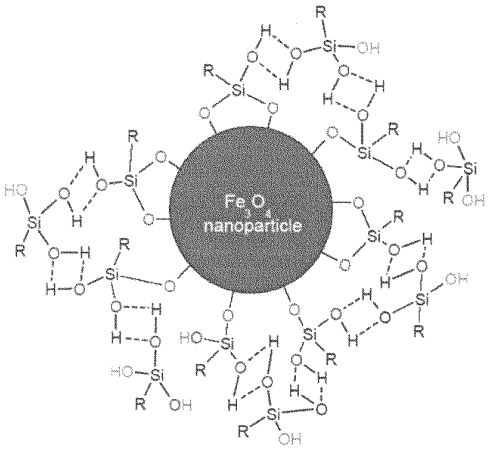

c. growth silicon layer

i) ≡Si-O-Si≡ bound establishment layer
ii) hydrogen bound establishment layer
iii) unoccupied hydrolysable -OH groups

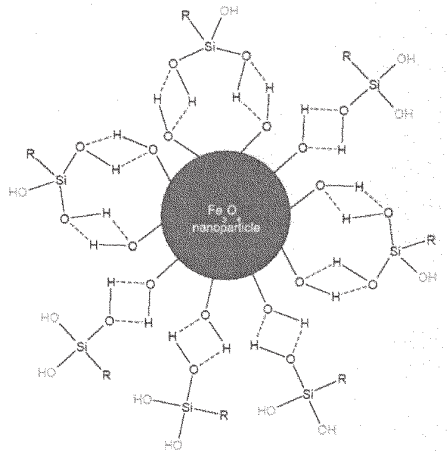

b. hydrogen bond establishment

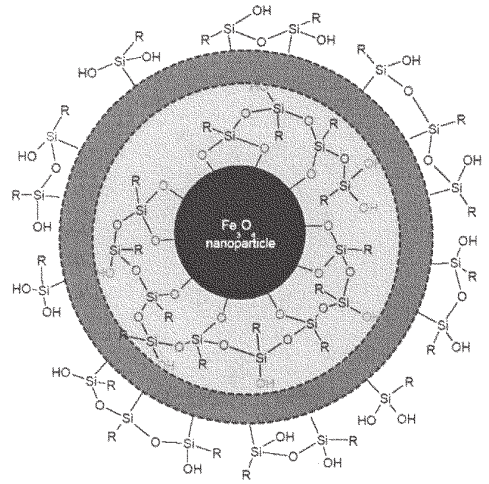

d. C1 layer growth on Fe_3O_4 surface as a function of time

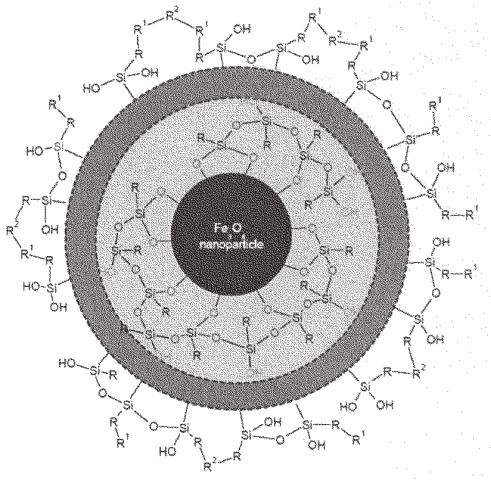

e. glutaraldehyde activation of external surface of C1

Fig.2. General scheme proposed for the physical and chemical processes involved in the nucleation, growth and biochemical activation of the C1 polimeric layer deposited on the surface of the Fe_3O_4 nanoparticles in accordance with the experimental obtained data. R = [-$(CH_2)_3$-NH_2] ; R^1 = [CHO-$(CH_2)_3$-CHO] ; R^2 = [=CH-$(CH_2)_3$-CH=]

Fe_3O_4 synthesis and ferofluidization

Fe_3O_4 nanoparticle suspension has been obtained through $FeCl_3$ (8.58g) and $FeCl_2$ (23.275g) coprecipitation [5], Fe^{2+}/Fe^{3+}=1:2 molar ratio, in the presence of NH_3 60mL (25%) and in a 1000 mL. reaction volume. Fe_3O_4 has been obtained according to the chemical equation (1):

$$FeCl_2 + FeCl_3 + 8NH_3 + 4H_2O \rightarrow Fe_3O_4 + 8NH_4Cl \qquad (1)$$

The coprecipitation reaction lasted for 30 minutes, the reaction temperature was 60^0C, and the ultrasound rate of stirring was of 55 KHz. The nanoparticle suspension has been separated through magnetic decantation by means of a magnet, and its *p*H reached the value of 7.5÷8 through sccessive washings and magnetic decantations. The nanoparticle stabilization [6] has been carried out through Fe_3O_4 treatment with azotic acid (100mL, 2,3M) for 15 min.

Additionally the Fe_3O_4 suspension has been treated with sodium citrate tribasic [7,19] for 15 min in order to passivise [8] the synthetised nanoparticle surface and to diminish the electric charge superficial density distributed on the Fe_3O_4 surface.

Fe_3O_4 nanoparticle coating in polymeric nanolayers of the C1 type

C1 has been deposited on the Fe_3O_4 surface through the cohydrolysis of 14mL (3-aminopropyl)-triethoxysilane ($C_9H_{23}NO_3Si$) according to the chemical reactions presented in figure 2 (eq. a, b, c, d).

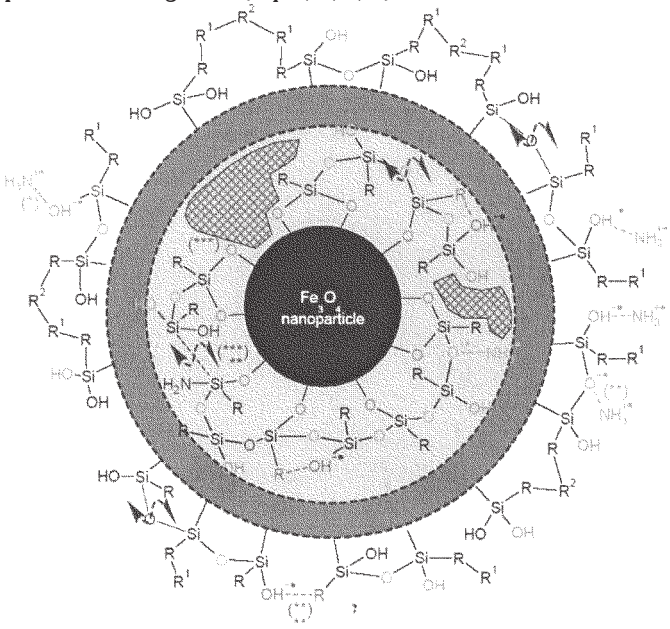

Fig.3 Chemical links likely to be established during the synthesis and growth of the C1 layer processes, and with an essential role in the distribution of physical and chemical characteristics on the surface and in the depth of C1 layer
(*) adsorbtion points of NH_3 through electrostatic links and the formation of new ones, of NH_3-OH type;
(**) electrostatic adsorbtion points of NH_3 around the ≡Si-O- Si ≡ links and the formation of others of ≡Si-(ONH_3)-Si ≡ type;
(***) freely formed space in polymerization network
(*) formation points of hydrogen links between –NH_2 and -OH
(***) ≡Si-(ONH_3)-Si ≡ link breaking points and the formation of new ones of ≡Si-OH and ≡Si-NH_2 type under local electrostatic tension pressure and polymer network inner energy

The reaction took place in a 1000mL mixture made up of: 480mL absolute etilic alcohol, 50mL NH_3-25%, ~4g Fe_3O_4 and distilled water.

The reaction lasted for 120 min and 30 mL of sample were taken every 15 min. The reaction temperature was of 60^0C, and the ultrasound stirring rate was of 55KHz. The sample pH reached the value of 7.5-8 through distilled water washing.

Fe_3O_4 nanoparticle activation with glutaraldehyde

The C1 nanoparticle suspension obtained in the previous stage has been added to a reaction mixture of 1000 mL made up of distilled water, 7mL glutaraldehyde ($C_5H_8O_2$) and 4mL NaOH. The pH of the initial mixture has reached the value of 12. The reaction lasted for 60 min at a temperature of 59^0C and a stirring rate of 55KHz. The glutaraldehyde biochemically activated suspension [9] was washed with 100mL NaCl (0.2M) and with distilled water towards the end of the process.The *p*H of the suspension prepared for subsequent uses reached the value of 7÷8.

Results and discussions

Fe_3O_4 nanoparticles have been synthetised [10], coated in a $n[SiO_{1.5-\gamma}\text{-}(CH_2)_3(NH_2)](NH_2)_{n\delta}$ polymeric layer and biochemically activated [11] with glutaraldehyde in order to test the biochemical fixing capacity. The reaction of nanoparticles obtained has ensued sequentially according to figure 2.

The C2 nanostructure obtained in the third stage of the synthesis has been separated with the help of a magnet. The *p*H of the suspension has been stabilised at the value of 7,5-8. The compositional and morphological analyses of Fe_3O_4-$n[SiO_{1.5\gamma}\text{-}(CH_2)_3(NH_2)](NH_2)_{n\delta}$ have been carried out through scanning electronic microscopy (ESEM) and transmission electronic microscopy [12] (TEM). The theoretical structure of the C1 coverage polymeric layer [13] is modelled by the chemical formula $nSiO_{1.5}\text{-}(CH_2)_3NH_2$. The γ and δ parametres have been subsequently introduced to explain deviations from the theoretical structure model noticed as a result of the analyses.The γ parameter has been introduced to correct the deviations from the theoretical condensation process of (3-aminopropyl)-triethoxysilane (fig.2 b), c)). The insertion of this parameter has been imposed by the analysis of the characteristic X ray spectra which show a significant difference between the oxygen and the silicone quantities identified in the nanostructure.

The δ parameter models the sum of the amino groups, of the -NH_2, NH_3 şi NH_4OH type coming from the ≡Si-$(CH_2)_3NH_2$ links which cannot be hydrolised and the NH_3 fixed in the structure flaws of the polymeric layer through hydrogen links, elctronic polarization, difussion [14,15] etc (fig.3). The ε (ε ≤δ) parameter models the superficial density of biological cross-linked molecules on the nanostructure surface. This parameter will be dealt with in a subsequent paper.

The analysis of the X ray spectra characteristic to the Fe_3O_4-$n[SiO_{1.5\gamma}\text{-}(CH_2)_3(NH_2)](NH_2)_{n\delta}$ (C2)

The X ray spectra characteristic to the elements found in the C1 structure are condensed in fig.4. The eight spectra correspond to the eight samples taken every 15 min, for two hours, during the deposition process of the silicone layer.

Tabel 1 presents the procentual atomic and mass concentrations of the elements identified in C1. The carbon spectral lines come from the ≡Si-$(CH_2)_3NH_2$ chemical links and from the carbon layer on which were deposed samples to be analysed. These lines do not give useful information concerning the NH_2 groups fixing mechanisms because

Crt.	N		O		Si		Fe		C	
%	Wt%	At %	Wt%	At %	Wt %	At %	Wt %	At %	Wt %	At %
P1	0.00	0.00	21.05	17.14	1.23	0.57	2.36	0.55	75.36	81.74
P2	1.18	1.18	22.78	19.89	3.44	1.71	7.90	1.98	64.70	75.25
P3	1.69	1.58	20.74	16.92	0.56	0.26	2.90	0.68	74.11	80.56
P4	1.45	1.43	26.57	22.82	2.75	1.35	5.10	1.25	63.72	72.91
P5	2.04	2.10	33.92	30.53	7.05	3.62	4.21	1.09	51.74	62.04
P6	2.34	2.27	25.96	22.05	1.95	0.94	3.64	0.89	64.53	73.00
P7	0.54	0.52	26.62	22.52	2.21	1.06	3.98	0.96	66.38	74.80
P8	1.53	1.45	16.98	14.12	2.88	1.36	2.71	0.65	73.35	81.28

Tabel 1
Fe, Si, N AND O CONTENT IN C1 (ESEM - PHILIPS XL30)

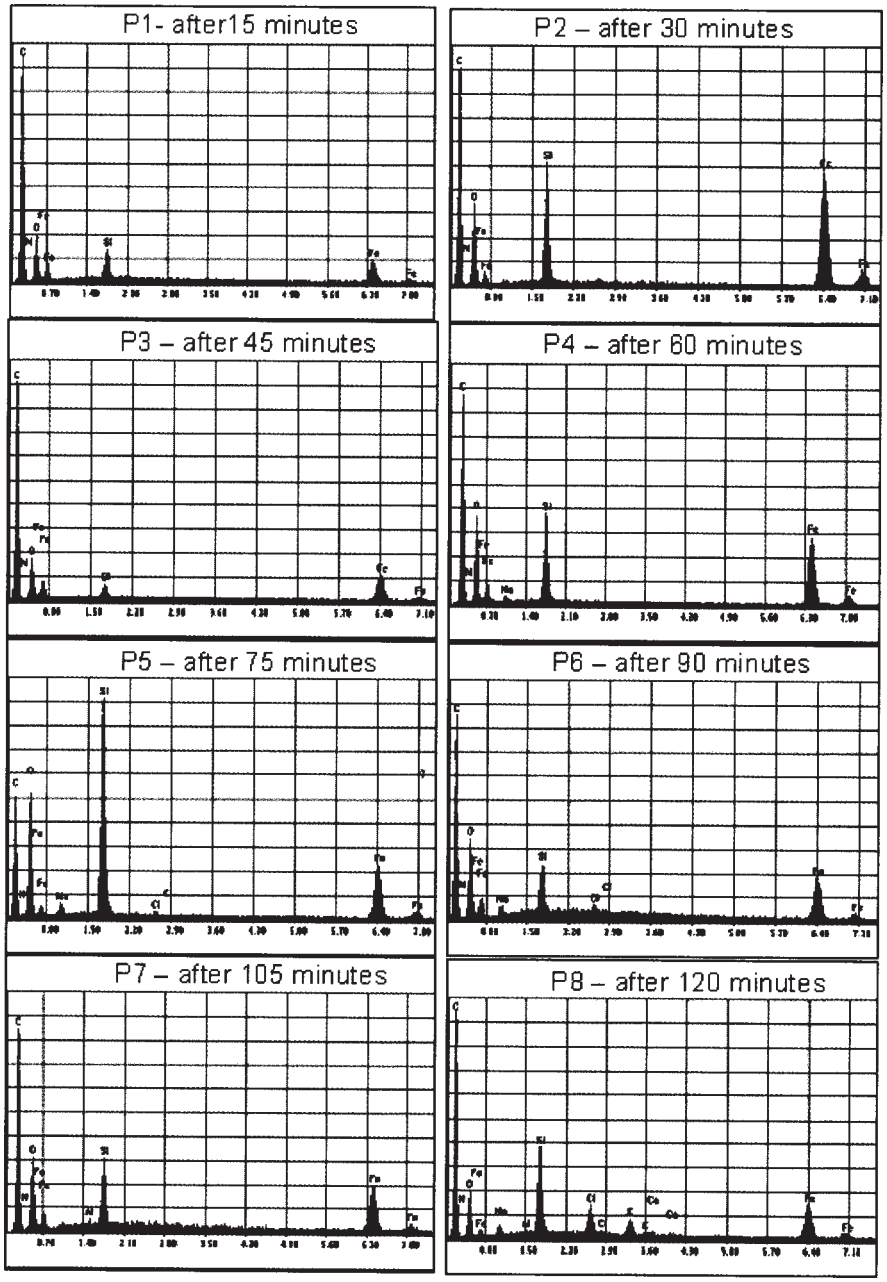

Fig.4. Characteristic X ray spectra emitted by the elements which make up C1

the C content is not constant in comparison with the focus area of the scanning electron beam.

According to the chemical process shown in figure 2, the theoretical ratio between Si, O and N in the process of silicone coating of the magnetite nanoparticles, should be: Si/O/N=1:1.5:1. The X ray spectra indicate the fact that the oxygen quantity is much higher than the theoretical one (fig.2, a), b)), and the nitrogen quantity fluctuates around the theoretical value (table 1).

These inconsistencies can be explained if one admits the fact that in the tridimensional network of C1 electrostatic tensions are generated due to the bonds of the ≡Si-OH- - - NH_3, ≡Si-(ONH_3)-Si≡, -NH_2- - -(HO)- (fig.3/*, **, **) type. An important role in the molecular chemosorbtion with low molecular mass is played by the free space bags (fig.3/***), unoccupied by the atoms or the molecules which make up C1. The holes in the molecular network of the C1 layer occur due to the surface flaws (e.g. the specific surface orientation), the group number – OH which can be hydrolised and which determine the policondensation degree of $C_9H_{23}NO_3Si$, the orientation in space of the links of the ≡Si–$(CH_2)_3NH_2$ which cannot be hydrolised type [16].

The ≡Si–C≡ bonds are responsible for the fluctuation of the condensation degree and for the Si/O variation ratio, according to the physical and chemical synthesis parameters, the length and the ramification degree of the carbon chain which bonds directly to the silicone. The

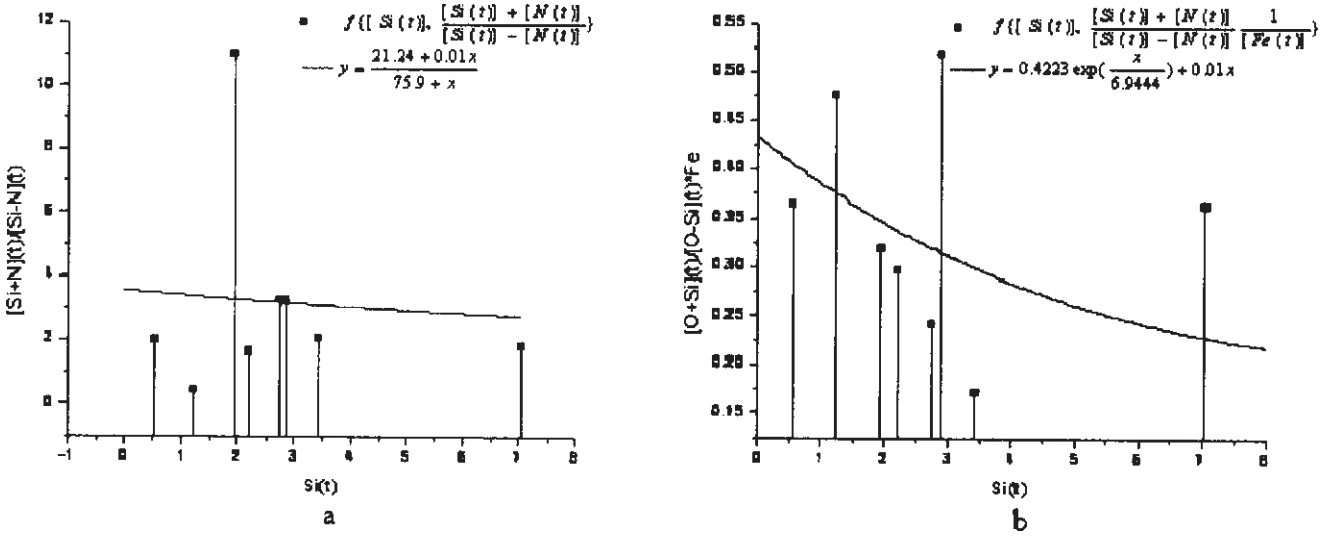

Fig. 5. The kinematics of the C1 polymeric layer growth on the magnetite surface 5a – the relative rate of $n[SiO_{1.5ā}\text{-}(CH_2)_3(NH_2)](NH_2)_{nā}$ on the Fe_3O_4 surface; 5b – the normed rate of $n[SiO_{1.5ā}\text{-}(CH_2)_3(NH_2)](NH_2)_{nā}$ acumulation on the Fe_3O_4 surface (the norming is in accordance with the Fe concentration in the magnetite nanoparticle)

internal tensions generated by the bonds which cannot be hydrolised model the γ [$\gamma\in$ (0, 1.5)] ratio concerning the ≡Si–O–Si≡ bond formation through the reorientation of the adjacent silicone atoms.

Some of the ≡Si–O–Si≡ bonds can break under the action of the electrostatic and mechanical tensions, forming new bonds of the ≡Si-OH- and ≡Si-NH_2 $^{**}_{*}$ type [17]. The bonds of the *, ** and $^{**}_{**}$ type are hydrogen bonds established in the growth stage of the C1 layer and subsequently integrated along with its growth. This type of bonds can also be established through NH_4OH diffusion in the depth of the already deposited polymer layer, or through internal structural reshaping occurring along with the variation of the local physical factors.

The graph in figure 5 (5.a) shows that δ grows slowly, along with n's growth. From the numerical simulation it ensues that the number of amino groups chemically and physically absorbed in the network and on the surphace of the C1 polymeric layer varies according to an approximately linear relation (fig. 5, 5.a). The variation of the physical and chemical absorbtion degree of amino groups can be explained through the fact that along with the volume growth of C1 the number and size of vacant spaces where these groups can fix through infiltration also grow. The graph in figure 5 (5.b) shows the time variation of the relative difference between the oxygen and silicone percents. The distribution function is exponentially and lineary combined. One can notice that it tends asimtotically towards the maximum theoretical value of the Si/O=1/1.5 (γ=1) ratio. The graph intersection with the y axix will give the oxygen quantity coming from the iron oxyde and it corresponds to the beginning of the reaction [f(Si)=0], when the oxygen quantity comes only from the magnetite cores.

The introduction of auxiliary physical and chemical processes, according to the theoretical diagram in figure 3, is necessary in order to explain the experimental results which are being presented in figure 7. In other words, the acceptance of this type of processes (identified in the diagram in figure 3 under the form of [$*$, $**$, $***$, $^{**}_{**}$, $^{***}_{**}$]) explains and models a series of physical and chemical processes, such as: i) excellent structural time stability of structures of the C2 type ii) excellent chemical stability [18] of the C1 structure in relation to the secondary hydrolysis processes iii) chemical time stability of the

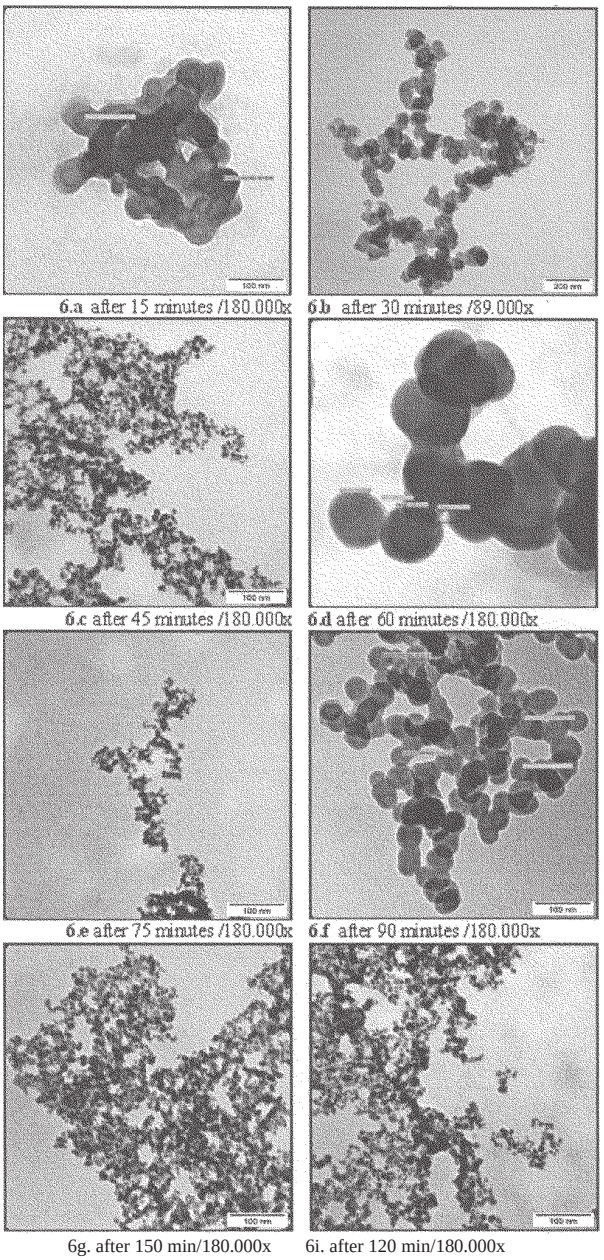

Fig. 6. Pictures of C2 in different moments of the deposition stage of the C1 layer

biologically activated surface, in relation to the 'auto' biological linking.

The samples presented in fig.7 were taken 30 days after carrying out the chemical syntheses analysed in this paper and support the hypotheses drawn in this study.

The microorganisms on which the C2 nano/microstructures were fixed through crossed biological linking, are part of the environmental microbiological flora and constitute a typical instance of uncontrolled biological and chemical crossed binding with a wide fixing spectrum. The pictures in fig. 7 (a, b) were obtained by using the Philips S208 (80 kV acceleration tension, 3 spot, 19 μA beam current and Olympus camera) electronic microscope.

After having morphologically and structurally analysed the patterns formed on the microorganism surface, one can draw the following conclusions: i) the microorganism surface presents areas which have high chemical affinity towards the C2 chemically activated surface ii) the C2 fixed on the microorganism surface have a discrete structure (it fixes as C2 nano/microparticles, separately or in small conglomerations / e.g. 2-3 C2 individual structures). The explanation of these experimental data compels one to admit that the biochemically active surface of C2 structures is saturated with chemical groups of the same type (most of the aldehyde type), so that between the C2 particles electostatic repulsion should appear or stable chemical bindings should not be formed.

The analysis of the C2 nanoparticle morphology

The establishment of the morphology of the magnetite nanoparticles coated in the C1 polymeric structure plays an important part in the correct establishment of the chemical mechanisms of deposition of the coating layer [19] as well as in the -NH_2 distribution in the depth and on the C1 surface.

Figure 6.a÷fig.6.i show pictures of C2 taken with Philips S208 transmission electonic microscope in different stages of the controlled deposition stage of the C1 layer.

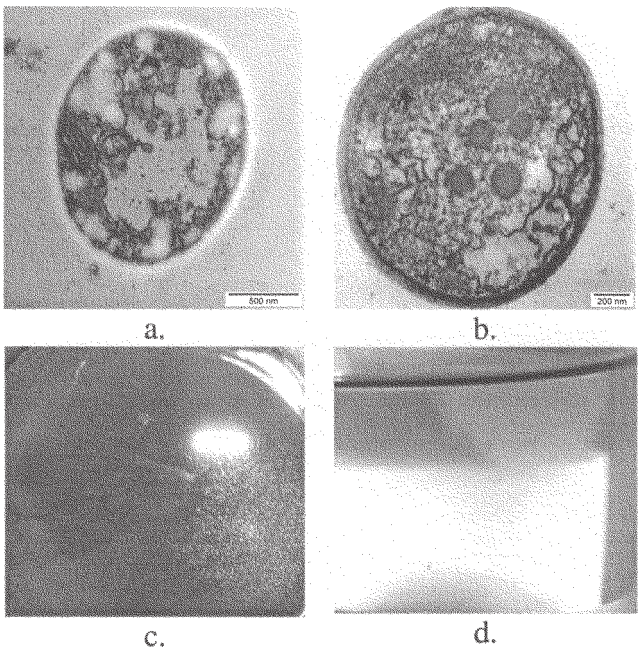

Fig.7 Pictures of the saprophyte bacterial flora (c, d) grown directly on the C2 underlayer, as well as the TEM method analysis of the fixing manner of C2 on the microorganism surface (a, b)

The TEM analysis indicates the fact that the synthetised nanoparticles are structurally made up of C1 and C2, have a well defined spherical shape and are visibly delimitated from the adjacent nanoparticles. One can notice that the C1 layer is uniformly distributed and has a thickness distribution between 1÷10nm. The study of the C2 morphology shows that in the C1 coverage stage polymeric bridges were formed between the nanoparticles that were subject to the coverage process. Most likely, these bridges are due to the gradients and the stirring fluctuatiuons in the condensation process of (3-aminopropyl)-triethoxysilane. It is important to mention that the silane co-hydrolysis and the co-condensation processes also lead to the formation of non-magnetic C1 nanoparticles in a relatively important quantity. Therefore, it ensues that the fixing of the C1 layer on the magnetic Fe_3O_4 only takes place through the (3-aminopropyl)-triethoxysilane hydrolysis with water molecules associated to the magnetite nanoparticles, while the growing process of the C1 layer takes place only through cohydrolysis [20] of –OH chemical groups of $(EtO)_3Si(CH_2)_3NH_2$ [fig.2, a), b), c) and fig.3].

Conclusions

As a result of the syntheses which have been carried out we have obtained Fe_3O_4 nanoparticles coated in polymeric layers of the C1 type, enriched with amino groups distributed on the surface and in the depth of the coating layer, and which have interesting characteristics in point of biochemical fixing. We have also investigated the absorbtion physical and chemical mechanisms of the amino groups in the C1 polymeric structure and we have determined the relative analytical relations which dictate the distribution process of the $(NH_2)_{n\delta}$-$(GL)_{n\varepsilon}$ fraction fixed on the C1 surface. The $(NH_2)_{n\delta}$ distribution was carried out according to time.

The TEM and ESEM analyses show that the synthetised suspension has a high stability in unpolar media of biological interest (fig.7). The graphs in figure 5 (5.a, 5.b) indicate a much higher variation in time of the degree of enrichment with oxygen coming from the uncondensed –OH groups of the C1 layer, as compared to the degree of enrichment with the (-NH_2, NH_3) amino groups of the same layer. The analytical results we have obtained demonstrate that the physical and chemical characteristics implanted to the structures we have studied, can be handled accordingly if we control the synthesis physical and chemical parameters [21].

This experimental data was feasible thanks to 31-001/2007 and 81-002/2007 projects, inside PNII research program

References

1. KIRSCHVINK, J., L., JONES, D., S., MACFADDEN B. J., Magnetite biomineralisation and magnetoreception in organisms, **1**, Ed. Plenum Press N.Y., 1985, p. 43
2. HÄFELI, U. O., PAUER, G. J., J. Magn. Magn. Mater., **194**, 1999, 76-82.
3. TOURINHO, F., A., FRANCK, R., MASSART, R., PERZYNSKY, R., Progr. Colloid Polym Sci., **79**, 1989, p. 128.
4. SELLMYER, D., SKOMSKI, R., Advanced Magnetic Nanostructures, chapter 3, Springer, 2006
5. TOURINHO, F., A., FRANCK, R., MASSART, R., J. Mater. Sci., **25**, 1990, p. 3249
6. DAVIES, K., J., WELLS, S., CHARLES, S., W., J. Magn. Magn. Mater., **24**, 1993, p. 122.
7. MARCHAND, A., FOREL, M., T., METKAS, F., VALADE, J., J. Chim. Phys., **61**, 1964, p. 343

8. DELTCHEFF, C., R., FRANCK, R., CABUIL, V., MASSART, R., J. Chem. Res. (S), 1987, p. 126
9. GRUTTNER, C., TELLER, J., J. Magn. Mater., **194** , nr. 1-3, 1999, p. 8
10. BLUM, E., MAIOROV, M., M., Magnetic Fluids, Walter de Gruyter (Ed.), Berlin, 1997
11. HÄFELI, U. O., SCHÜTT, W., TELLER, J. et al, Scientific and clinical applications of magnetic carriers, **1st** Ed., Plenum, New York, 1997
12. BOJIN, D., MICULESCU, F., BUNEA, D., MICULESCU, M., Scanning electron microscopy and applications, Ed. Agir, Bucureşti, 2005
13. PLUEDDEMANN, E., P., Silane Coupling Agents, **2nd** Ed., Plenum Press - New York and London, 1991
14. ABRAMS, L., SUTHERLAND, J., W., J. Phys. Chem., **73**, 1969**,** p. 3160
15. GRIFFITHS, D., W., L., HALLAM, H., E., THOMAS, W., J., Trans. Faraday Soc., **64**, p. 1968,3361
16. MUKBANIANI, O., V., ZAIKOV, G., E., Copolymers: Synthesis, Properties, Application, VSP, Utrecht, Boston, 2003
17.MARCHAND, A., FOREL, M., T., METKAS, F., VALADE, J., J. Chim. Phys., **61**, 1964, p. 343
18.HADARUGA, D., I., HADARUGA, N., G., RIVIS, A., GRUIA, A., PINZARU, I., A., Rev. Chim. (Bucuresti)., **58**, nr. 11, 2007, p. 1009
19. GU, J., YANG, W., DENG, Y., WANG, C., FU, S., small, **1**, 2005, p. 737
20. DENG, Y., WANG, C., SHEN, X., YANG, W., JIN, L., GAO, H., FU, S., Chem. Eur. J., **11**, 2005, p. 6006
21. R. M. CORNELL, The Iron Oxides: Structures, Properties, Reactions, Occurence and Uses, 1996, VCH, Weinheim

Manuscript received: 17.06.2008